Kinetic Evidence for the Redox Cycling of Manganese(II,III) in the Presence of $^{-}ON(NO)SO_3^{-}$ in Aqueous Media

Frans F. Prinsloo,[a] Jakobus J. Pienaar[a] and Rudi van Eldik*,†,[b]

[a] *Department of Chemistry, Potchefstroom University for Christian Higher Education, 2520 Potchefstroom, South Africa*

[b] *Institute for Inorganic Chemistry, University of Witten/Herdecke, 58448 Witten, Germany*

Redox cycling of $Mn^{II/III}$ in the presence of $^{-}ON(NO)SO_3^{-}$ in the absence and presence of oxygen was studied by following the increase and decrease of Mn^{III} spectrophotometrically as a function of [$^{-}ON(NO)SO_3^{-}$], [Mn^{III}], [Mn^{II}] and pH. The autoxidation reaction exhibits typical autocatalytic behaviour in which the induction period depends on the concentrations of Mn^{III} and $^{-}ON(NO)SO_3^{-}$. Under acidic conditions the reaction does not take place in the absence of Mn^{III} or O_2. The concentrations of O_2, Mn^{II} and $^{-}ON(NO)SO_3^{-}$ determine whether only oxidation of Mn^{II} to Mn^{III}, or reduction of Mn^{III} to Mn^{II}, or both in one or two redox cycles is observed. Preliminary simulations of some of the observed kinetic traces are presented.

Metal-catalysed oxidation reactions of SO_2 and NO_x species in aqueous solution have attracted the attention of chemists from a variety of disciplines[1–14] due to the importance of such processes both in the atmosphere and in wet limestone flue-gas desulfurization (FGD) systems. A series of studies on the catalytic effect of metal ions and complexes of Fe,[15–19] Co[20] and Mn[21] revealed that the metal-catalysed autoxidation of sulfite and the sulfite-induced autoxidation of the different metal ions can be explained by a common mechanism. In this the trivalent metal ion is reduced by sulfite to produce a sulfite radical which initiates the formation of sulfate and peroxomonosulfate radicals in the presence of O_2. These radicals are responsible for the reoxidation of the metal ion to the trivalent state in order to complete the catalytic cycle.[22]

Our current interest concerns the redox behaviour of manganese in the presence of nitrogen–sulfur compounds, which are formed in FGD systems *via* the key compound $HON(SO_3)_2^{2-}$. The latter is formed in solution *via* the reaction of nitrite with sulfite[23–26] or NO with HSO_3^{-} in the presence of Fe^{II} according to a Boedeker-type mechanism.[27,28] Under acidic conditions, $HON(SO_3)_2^{2-}$ is unstable and decomposes to $HONH(SO_3)^{-}$. The dianion $^{-}ON(NO)SO_3^{-}$ can be formed in FGD systems *via* base hydrolysis of $HONH(SO_3)^{-}$,[29] its reaction with NO_2^{-},[30] or the reaction of NO with sulfur(IV) oxides.[31]

In a recent kinetic study of the reduction of Mn^{III} by a variety of nitrogen–sulfur compounds[26] we showed that the results could account for some typical observations made in FGD systems. Limited information on the influence of such compounds on the possible oxidation of divalent metal ions has appeared in the literature. In a study on the reaction of chelated iron(II) nitrosyl complexes with sulfite and hydrogensulfite ions, Littlejohn and Chang[32] reported a mechanism for this reaction which involves the oxidation of $Fe^{II}L$ [L = a poly(amino-carboxylate)] by $^{-}ON(NO)SO_3^{-}$. In much the same way as our earlier study the sulfite-induced autoxidation of Mn^{II} in azide medium,[21] we have now made a systematic kinetic analysis of the possible oxidation of Mn^{II} by $^{-}ON(NO)SO_3^{-}$ in basic and acidic solutions. We report for the first time kinetic evidence for the redox cycling of Mn^{II} and Mn^{III} in the presence of this dianion.

† *Present address:* Institute for Inorganic Chemistry, University of Erlangen-Nürnberg, Egerlandstrasse 1, 91058 Erlangen, Germany.

Experimental

All reagents were of analytical grade (Merck and Fluka) and deionized water was used to prepare all the solutions. Argon was used to deaerate the solutions where required. The dianion $^{-}ON(NO)SO_3^{-}$ was synthesized according to a literature procedure.[33] For measurements at high pH a carbonate buffer (0.025 mol dm^{-3}) was used to stabilize the solution pH. Eluents for the ion chromatographic analysis were prepared from sodium carbonate, tetrabutylammonium hydroxide and acetonitrile. The equipment used for this analysis and the selected experimental conditions under which it was performed were the same as those adopted before.[34] The UV/VIS spectra were recorded at constant time intervals on Hewlett-Packard 8452A diode-array and Cary spectrophotometers. These instruments were also used for kinetic measurements of slow reactions in their thermostatted (±0.1 °C) cell compartments. Fast reactions were followed on a Durrum D110 stopped-flow instrument. The instruments were run on-line with an IBM compatible personal computer, and the absorbance *vs.* time traces obtained from the OLIS KINFIT (OLIS Inc., Bogart, GA) set of programs were converted into a standard graphical format. The pH measurements were performed on a Metrohm 632 pH-meter equipped with a Sigma glass electrode.

Results and Discussion

The rate of spontaneous hydrolysis of $^{-}ON(NO)SO_3^{-}$[35–37] is plotted as a function of [H^+] in Fig. 1, from which it can be seen

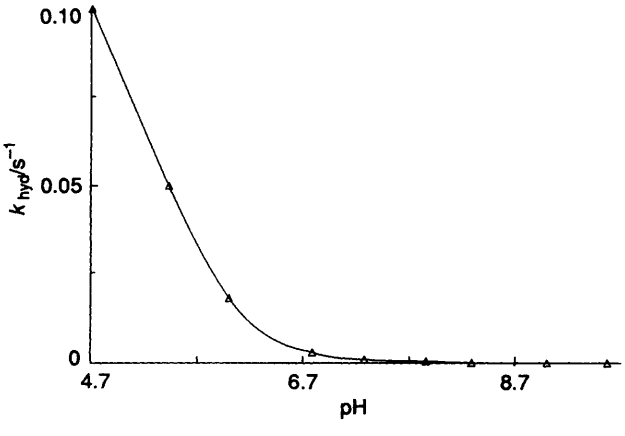

Fig. 1 The pH dependence of the rate of hydrolysis of $^{-}ON(NO)SO_3^{-}$

that the dianion is relatively stable in basic solution. On the other hand, Mn^{II} is readily oxidized by dissolved O_2 in basic solution.[38] Thus a typical experiment at high pH was executed by filling a tandem cuvette (under argon when required) with a deaerated solution of Mn^{II} at neutral pH and a buffered solution containing the dianion. Flue-gas desulfurization systems are generally operated at pH < 7 and it was therefore of interest to study the reaction at low pH as well. At pH < 7 both $^{-}ON(NO)SO_3^{-}$ and Mn^{III} are unstable. Based on our previous experience in azide media[21] and since the azide ion forms stable complexes with metal ions,[39,40] we stabilized Mn^{III} in this pH range by working in an azide medium. The $^{-}ON(NO)SO_3^{-}$ solutions were kept between pH 8 and 9 and were used immediately after preparation.

The first evidence for the oxidation of Mn^{II} by $^{-}ON(NO)SO_3^{-}$ was obtained when the possible influence of $HONH(SO_3)^{-}$ on the autoxidation of Mn^{II} at pH > 10.5 was studied. Under these conditions no azide was added to stabilize Mn^{III}. When $HONH(SO_3)^{-}$ is placed in an oxygen-saturated solution buffered at pH 10.5 and immediately mixed with a solution containing Mn^{II} a build-up of a product having λ_{max} = 260 nm is observed, after which Mn^{III} is formed (λ_{max} = 400 nm) (Fig. 2). The product having λ_{max} = 260 nm is $^{-}ON(NO)SO_3^{-}$, since it is known that $HONH(SO_3)^{-}$ undergoes base hydrolysis in the presence of oxygen[29] according to equation (1) as illustrated in Fig. 3.

$$O_2 + 3HONH(SO_3)^{-} + 4OH^{-} \longrightarrow NO_2^{-} + {}^{-}ON(NO)SO_3^{-} + 2SO_3^{2-} + 5H_2O \quad (1)$$

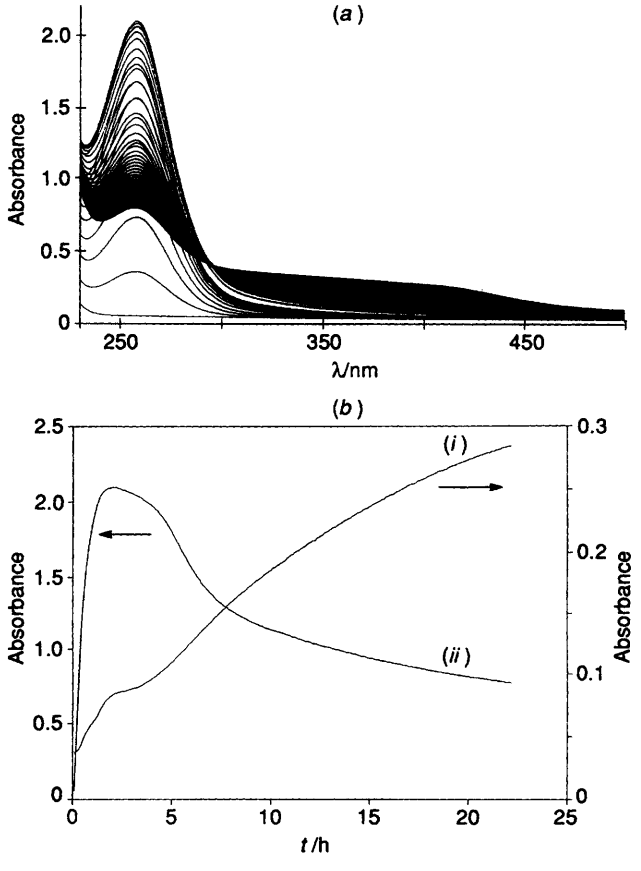

Fig. 2 (*a*) Spectral changes during the reaction of $HONH(SO_3)^{-}$ with Mn^{II}. Conditions: $[Mn^{II}] = 1 \times 10^{-4}$, $[HONH(SO_3)^{-}] = 1 \times 10^{-3}$ mol dm^{-3}; pH 10.5; 25 °C; $[O_2] \approx 6.25 \times 10^{-4}$ mol dm^{-3}; Δt = 360 s (first 10 spectra) and 1800 s (eleventh and subsequent spectra). (*b*) Absorbance *vs.* time traces at different wavelengths, *i.e.* λ = 260 nm (*i*) where the formation of $^{-}ON(NO)SO_3^{-}$ can be observed and 400 nm (*ii*) where the formation of Mn^{III} can be observed

The dianion has an absorption coefficient of 7000 dm^3 mol^{-1} cm^{-1} at 260 nm.[29] It could also be identified *via* ion chromatographic analysis of the hydrolysis products (Fig. 4). In agreement with a literature finding,[29] the ion chromatographic analysis also confirms the formation of NO_2^{-}, SO_3^{2-} and SO_4^{2-}. From Fig. 4 it is clear that NO_3^{-} and $HON(SO_3)_2^{2-}$ are also produced during the base hydrolysis of $HONH(SO_3)^{-}$. The formation of NO_3^{-} was accounted for in the initial net reaction,[29] but not in the overall reaction stoichiometry. We suggest that it can be formed according to Scheme 1.

$$^{-}ON(NO)SO_3^{-} \rightleftharpoons ONSO_3^{2-} + NO$$

$$2NO + O_2 \longrightarrow 2NO_2$$

$$2NO_2 \rightleftharpoons N_2O_4$$

$$N_2O_4 + 2OH^{-} \rightleftharpoons NO_3^{-} + NO_2^{-} + H_2O$$

Scheme 1

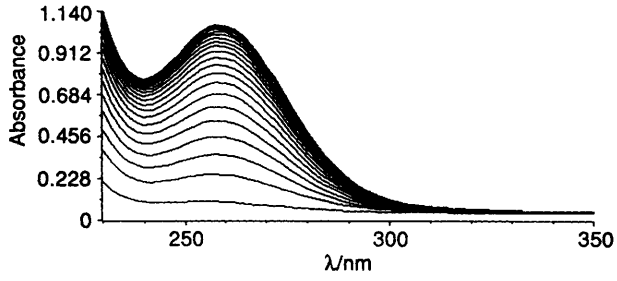

Fig. 3 Spectral changes during the base hydrolysis of $HONH(SO_3)^{-}$. Conditions: $[HONH(SO_3)^{-}] = 1 \times 10^{-3}$ mol dm^{-3}; pH 10.5; 25 °C; $[O_2] \approx 6.25 \times 10^{-4}$ mol dm^{-3}; Δt = 3600 s

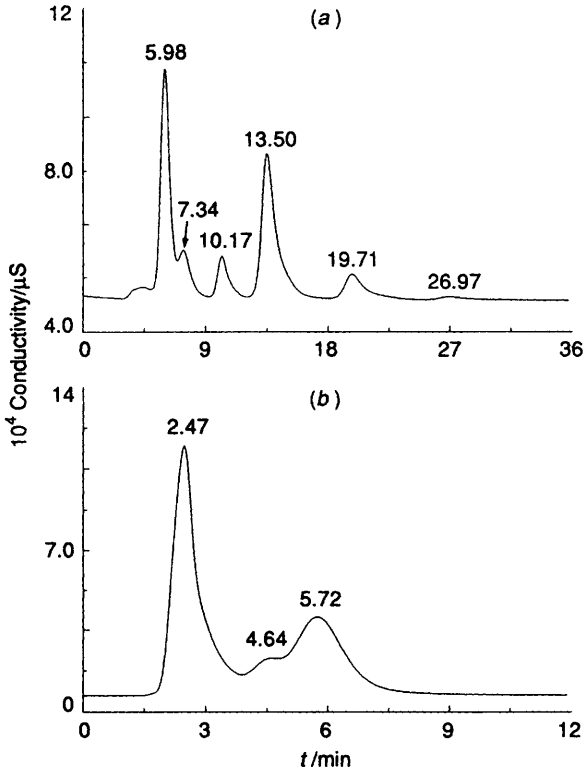

Fig. 4 Chromatograms of the products formed during the base hydrolysis of $HONH(SO_3)^{-}$. Conditions: pH 10.5; 25 °C; $[HONH(SO_3)^{-}] = 1 \times 10^{-3}$ mol dm^{-3}. (*a*) Obtained after 24 h of mixing, by ion permeation chromatography (IPC): *t* = 5.98, $HONH(SO_3)^{-}$, Cl^{-}; 7.34, NO_2^{-}; 10.17, NO_3^{-}; 13.5, SO_4^{2-}; 19.71, $HON(SO_3)_2^{2-}$; 26.97 s, $^{-}ON(NO)SO_3^{-}$. (*b*) Obtained after 3 h of mixing by IC: *t* = 2.47, $HONH(SO_3)^{-}$, Cl^{-}, NO_3^{-}, NO_2^{-}; 4.64 s, SO_3^{2-}; 5.72 s, SO_4^{2-}

Further support for oxygen consumption during reaction (1) was obtained by monitoring the concentration of dissolved oxygen with an oxygen-sensitive electrode (OXYTEC) during the course of the reaction.[41] It was found that the concentration decreased according to a first-order decay during the base-hydrolysis reaction.

The formation of $HON(SO_3)_2^{2-}$ in Fig. 4 is ascribed to the reaction of NO_2^- with SO_3^{2-}. It is expected that the rate of this reaction is slow,[30,42,43] and at high pH it becomes unfavourable compared to the oxidation of SO_3^{2-} by dissolved oxygen.

The increase in absorbance at 400 nm in Fig. 2(*a*) is ascribed to the formation of Mn^{III}. Acidification of such a solution with $HClO_4$ caused an immediate shift in the maximum to 460 nm, which is the characteristic absorption of aquated Mn^{III} in acidic solution.[44] The difference in these maxima is ascribed to the hydrolysis of Mn^{III} at pH 10.5 as compared to the hexaaqua species in acidic media. The exact nature of the hydrolysed manganese(III) species under our conditions is difficult to predict,[45] and could include $Mn(OH)_3$, MnO(OH), *etc.*

The build-up of Mn^{III} is preceded by an induction period during which $^-ON(NO)SO_3^-$ is formed in solution (λ = 260 nm) and partial oxidation of Mn^{II} occurs. The dianion then decomposes in two steps of which the second coincides with the formation of Mn^{III} [Fig. 2(*b*)]. The first part of this decomposition reaction can only be attributed to a concurrent formation and decomposition of the dianion. This hypothesis is further confirmed by the fact that this step coincides with the induction period, before any significant concentration of Mn^{III} is formed in solution. Noteworthy is the isosbestic point at λ = 296 nm which suggests a single reaction step between the dianion and Mn^{II} resulting in the formation of Mn^{III}. Ion chromatographic analysis of the products (Fig. 5) formed during this reaction indicated that sulfite, sulfate, $HON(SO_3)_2^{2-}$ and NO_3^- were formed. In contrast to the base hydrolysis of $HONH(SO_3)^-$, no NO_2^- could be detected. Its absence in the presence of Mn^{II} can be explained in two ways. First, oxidation of NO_2^- by Mn^{III},[46] formed due to the O_2 and $^-ON(NO)SO_3^-$-induced oxidation of Mn^{II},[39] cannot be ruled out. Secondly, it is also possible that, much in the same way as for the oxidation of iron(II) complexes by NO_2^-,[28] a Mn^{II}–$^-ON(NO)SO_3^-$ complex can be formed*,[11] (see further Discussion) which reacts with NO_2^-. This could result in the formation of Mn^{III}–$^-ON(NO)SO_3^-$ and NO. The latter can participate in further reactions with Mn^{II}–$^-ON(NO)SO_3^-$ and O_2 to produce $[Mn^{II}\{ON(NO)SO_3\}(NO)]$ and NO_2, respectively. The NO_2 can subsequently react with Mn^{II} (ref. 47) to produce NO_2^- and Mn^{III}.

These findings are not sufficient evidence to prove that $^-ON(NO)SO_3^-$ oxidizes Mn^{II} to Mn^{III}, since in basic solution the oxidation of Mn^{II} is induced by dissolved oxygen.[38] The reaction of $HONH(SO_3)^-$ with Mn^{II} in the absence of oxygen only results in the formation of different manganese(II) hydroxo species,[38] since $^-ON(NO)SO_3^-$ is only formed from $HONH(SO_3)^-$ in the presence of oxygen.[30,48] It must be kept in mind that the spectral changes reported in Fig. 2 differ completely from those observed for the autoxidation of Mn^{II}.[38] It was therefore necessary to investigate the oxidation of Mn^{II} in the presence of $^-ON(NO)SO_3^-$ under conditions where it does not occur at all when the dianion is not present in solution, *i.e.* with argon-saturated solutions.

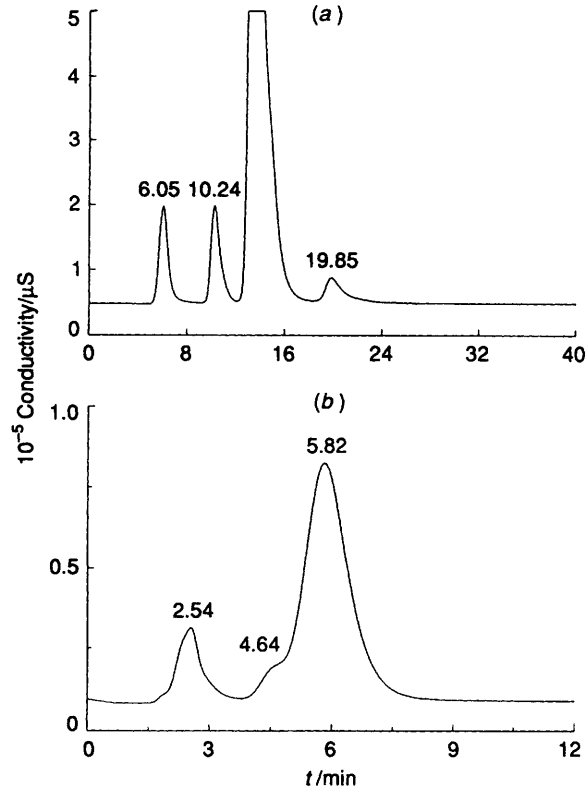

Fig. 5 Chromatograms of the products formed during the reaction of $HONH(SO_3)^-$ with Mn^{II}. Conditions: pH 10.5; 25 °C; $[HONH(SO_3)^-] = 1 \times 10^{-2}$ mol dm^{-3}. (*a*) Obtained by IPC: t = 6.05 s, $HONH(SO_3)^-$, Cl^-; 10.24 s, NO_3^-; 12–17 s, SO_4^{2-}; 19.85 s, $HON(SO_3)_2^{2-}$. (*b*) Obtained by IC: t = 2.54 s, $HONH(SO_3)^-$, Cl^-, NO_3^-; 4.64 s, SO_3^{2-}; 5.82 s, SO_4^{2-}

The dianion is unstable at pH 10.5 and hydrolyses to produce N_2O and sulfate.[49] At 25 °C and 0.025 mol dm^{-3} ionic strength the rate constant of this decomposition k_{dec} was measured as 1.4×10^{-4} s^{-1}, in good agreement with a previously reported value of 1.0×10^{-4} s^{-1} at pH 10.3.[49] Spectral changes upon mixing $^-ON(NO)SO_3^-$ with Mn^{II} in the absence of oxygen are illustrated in Fig. 6(*a*). These are very similar to the second part of the spectral changes observed when $HONH(SO_3)^-$ is mixed with Mn^{II} (Fig. 2), which confirms that $HONH(SO_3)^-$ first hydrolyses to $^-ON(NO)SO_3^-$ and then participates in the oxidation of Mn^{II}. The decomposition of $^-ON(NO)SO_3^-$, or Mn^{II}–$^-ON(NO)SO_3^-$, corresponds to the first part of the absorbance *vs.* time traces [Fig. 6(*b*)], since no build-up of Mn^{III} was observed during this interval and it coincides with the induction period. The rate constant was measured as 3×10^{-4} s^{-1}, which is larger than k_{dec} and confirms that the decomposition of $^-ON(NO)SO_3^-$ is accelerated by the presence of manganese(II) hydroxides. In Fig. 6(*b*) the second part of the absorbance *vs.* time trace at λ = 260 nm corresponds to the redox decomposition of the dianion, since it is accompanied by the formation of Mn^{III} observed at λ = 400 nm. Only sulfate was observed in an ion chromatographic analysis of the reaction mixture, which further supports the hydrolysis of the dianion as reported in the literature.[48]

According to reaction (1), base hydrolysis of $HONH(SO_3)^-$ in the presence of oxygen results in the formation of $^-ON(NO)SO_3^-$ and sulfite. We therefore also checked the oxidation of Mn^{II} to Mn^{III} by sulfite in Ar-saturated solution under the conditions of the present investigation. The results in Fig. 7 clearly demonstrate rapid hydrolysis of Mn^{II}, followed by slow conversion of Mn^{II} into Mn^{III} in the presence of sulfite. Literature data suggest the formation of $[Mn_2(OH)_3]^+$ under these conditions due to the limited solubility of $Mn(OH)_2$.[38,45] The observed spectral changes for the second part of the process

* Manganese(II) is a d^5 metal ion which causes weak, spin-forbidden, electronic transitions in the UV/VIS region, but due to the absence of crystal-field stabilization energy for this, normally high-spin, ion a weakly bonded complex is expected to be formed. This is also evident from the fact that Mn^{II} does not form strongly bonded complexes with typical ligands as do some of the later first-row transition-metal ions. At high pH hydroxide ligands themselves will be strongly bound and substitution inert, but they may induce a lability of the *trans*-water molecule. Thus the $[Mn(H_2O)_5(OH)]^+$ species is expected to be more substitution labile than is $[Mn(H_2O)_6]^{2+}$.

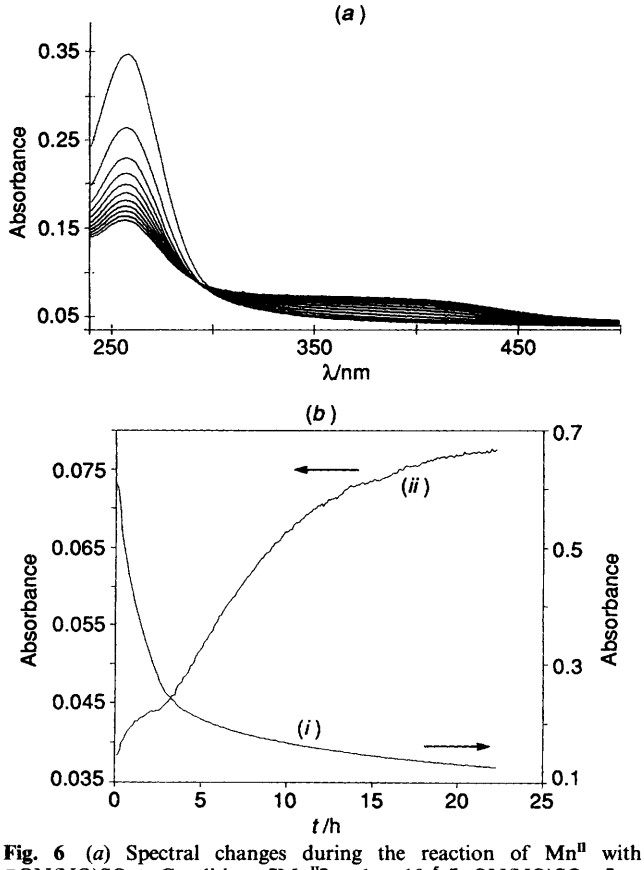

Fig. 6 (*a*) Spectral changes during the reaction of Mn^{II} with $^{-}ON(NO)SO_3^{-}$. Conditions: $[Mn^{II}] = 1 \times 10^{-5}$, $[^{-}ON(NO)SO_3^{-}] = 1 \times 10^{-4}$ mol dm^{-3}; pH 10.5; 25 °C; $[O_2] \approx 0$ mol dm^{-3}; between 240 and 500 nm; $\Delta t = 360$ s. (*b*) Absorbance *vs.* time traces at different wavelengths, *i.e.*, $\lambda = 260$ nm (*i*) where a decrease in $^{-}ON(NO)SO_3^{-}$ concentration can be observed and 400 nm (*ii*) where the formation of Mn^{III} can be observed

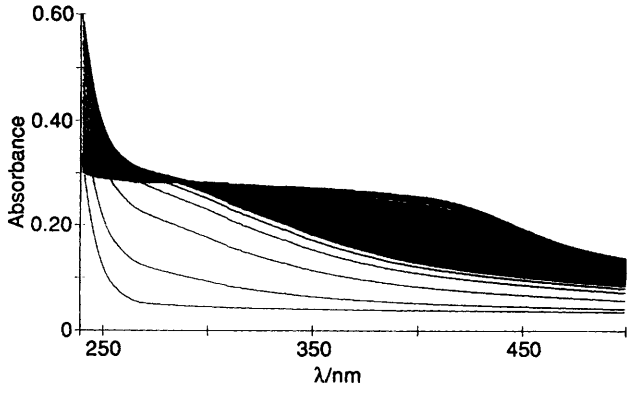

Fig. 7 Spectral changes during the reaction of Mn^{II} with sulfite. Conditions: $[Mn^{II}] = 1 \times 10^{-4}$ mol dm^{-3}, $[S^{IV}] = 2$ mmol dm^{-3}; pH 10.5; 25 °C; $[O_2] \approx 0$ mol dm^{-3}

are very similar to those in Fig. 2(*a*) and can therefore also account for the oxidation of Mn^{II} to Mn^{III}.

Subsequently, a systematic study of the possible oxidation of Mn^{II} by $^{-}ON(NO)SO_3^{-}$, at pH < 7, and in the presence of low concentrations of Mn^{III} was performed. Azide was used throughout these experiments to stabilize Mn^{III} in this pH range.[21] The UV/VIS spectra and the absorbance *vs.* time traces [Fig. 8(*a*) and 8(*b*)] indicate that upon mixing, complex formation between Mn^{II} and the dianion causes the maximum at 410 nm (due to the presence of Mn^{III}) to shift to 360 nm, after which Mn^{II} is oxidized to Mn^{III}. Under similar conditions, but in the absence of initially added Mn^{III}, complex formation was

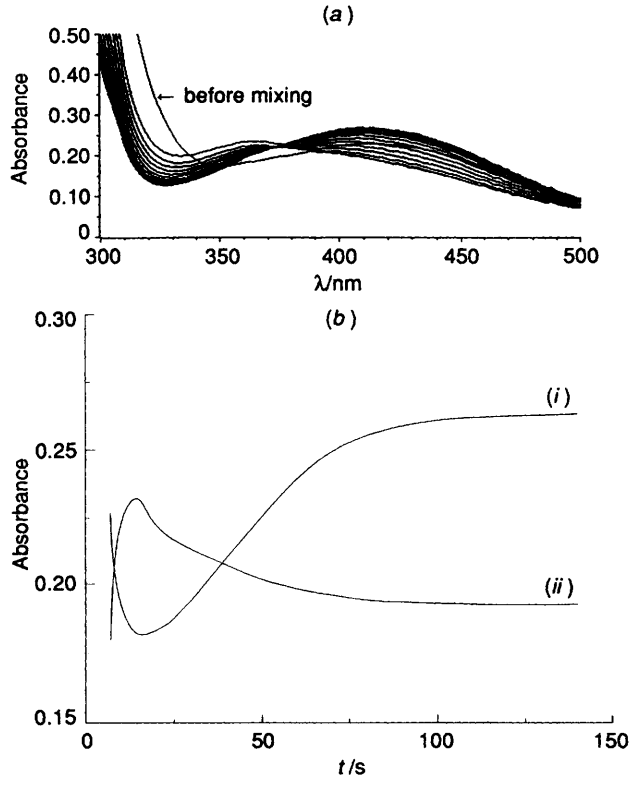

Fig. 8 (*a*) Spectral changes during the reaction of $^{-}ON(NO)SO_3^{-}$ with $Mn^{II/III}$. Conditions: $[^{-}ON(NO)SO_3^{-}] = 4$ mmol dm^{-3}; $[Mn^{II}] = 0.05$ mol dm^{-3}; $[N_3^{-}] = 0.5$ mol dm^{-3}; pH 6; 25 °C; $I = 0.6$ mol dm^{-3}; $[O_2] \approx 6.25 \times 10^{-4}$ mol dm^{-3}; $[Mn^{III}] = 0.05$ mmol dm^{-3}, $\Delta t = 7$ s. (*b*) Absorbance *vs.* time analysis at different wavelengths, *i.e.* $\lambda = 360$ (*i*) and 420 nm (*ii*)

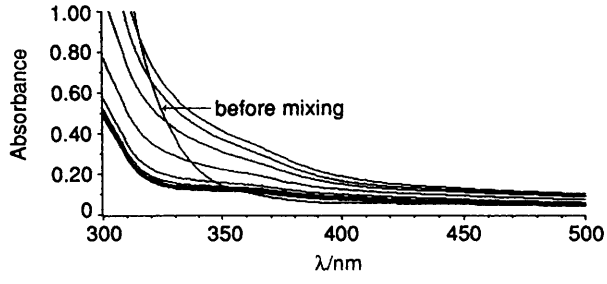

Fig. 9 Spectral changes during the reaction of $^{-}ON(NO)SO_3^{-}$ with Mn^{II}. Conditions: $[^{-}ON(NO)SO_3^{-}] = 4$ mmol dm^{-3}; $[Mn^{II}] = 0.05$ mol dm^{-3}; $[N_3^{-}] = 0.5$ mol dm^{-3}; pH = 6; 25 °C; $I = 0.6$ mol dm^{-3}; $[O_2] \approx 6.25 \times 10^{-4}$ mol dm^{-3}

again observed at 365 nm but no further oxidation of Mn^{II} could be seen (Fig. 9). The product formed at $\lambda = 365$ nm most probably is Mn^{II}–$^{-}ON(NO)SO_3^{-}$, since the formation of $Mn^{II}(NO)$ or $Mn^{II}(SO_3)$ is ruled out by the fact that when the experiment in Fig. 8(*a*) was repeated with NO or SO_3^{2-} as reactant species no oxidation of Mn^{II} in the case of NO or product formation at 365 nm in the case of SO_3^{2-} was observed. A series of kinetic measurements revealed no significant influence of the concentration (1×10^{-4}–3×10^{-4} mol dm^{-3}) of $^{-}ON(NO)SO_3^{-}$ on the observed rate constant for the formation of Mn^{III} (0.08 ± 0.01–0.11 ± 0.01 s^{-1} at 25 °C, pH 6 and $[Mn^{III}] = 5 \times 10^{-5}$ mol dm^{-3}). Under the same conditions, but with a higher $[Mn^{III}]$, the observed rate constant increases dramatically (1.95 ± 0.06–1.99 ± 0.01 s^{-1} at $[Mn^{III}] = 1 \times 10^{-4}$ mol dm^{-3}). This confirms that Mn^{III} is the active species during the autocatalytic process.

A detailed quantitative kinetic investigation of the $^{-}ON(NO)SO_3^{-}$-induced oxidation of Mn^{II} was then performed in which

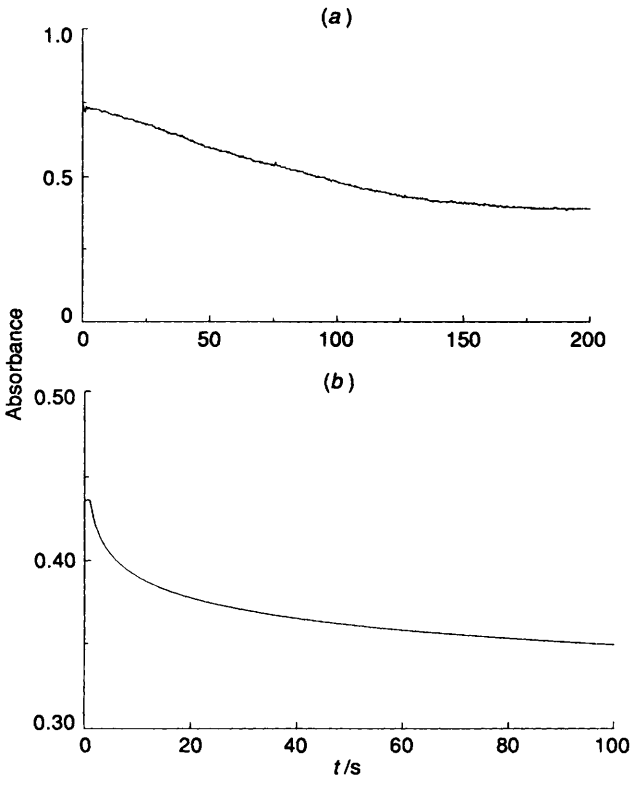

Fig. 10 Absorbance *vs.* time plots during the reaction of $^{-}ON(NO)SO_3^{-}$ with $Mn^{II/III}$ in the absence of oxygen. Conditions: $[Mn^{II}]$ = 0.025, $[N_3^{-}]$ = 0.5 mol dm^{-3}; $[^{-}ON(NO)SO_3^{-}]$ = 8 mmol dm^{-3}; 25 °C; I = 1.0 mol dm^{-3}; λ = 420 nm; pH 6 (*a*) or 7 (*b*)

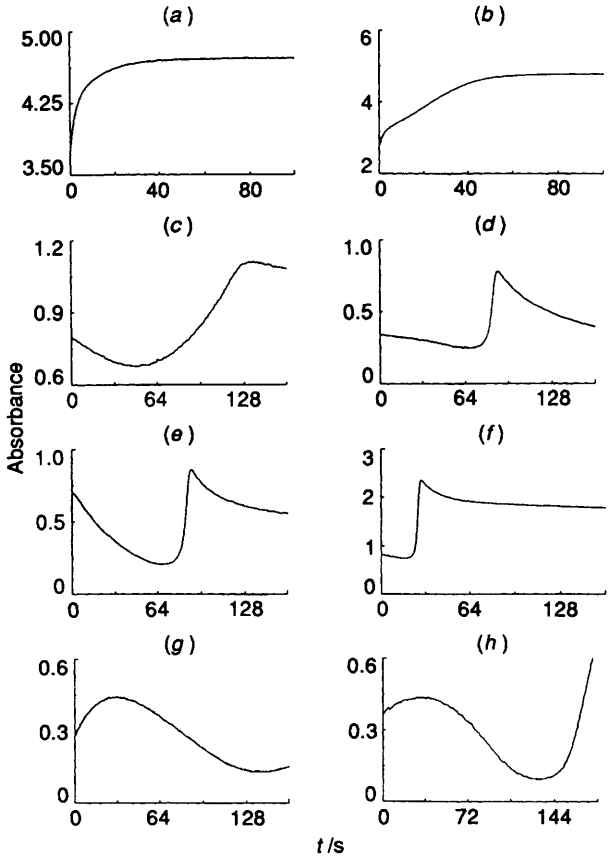

Fig. 11 Typical absorbance *vs.* time plots to demonstrate the occurrence of two reaction cycles during the reaction of $Mn^{II/III}$ with $^{-}ON(NO)SO_3^{-}$ in aqueous media. Conditions: $[N_3^{-}]$ = 0.5 mol dm^{-3}; pH 6 [(*a*)–(*f*)] or 7 [(*g*), (*h*)]; I = 1.0 mol dm^{-3}; $[O_2] \approx 6.25 \times 10^{-4}$ mol dm^{-3}; 25 °C; λ = 420 nm; 0.1 mmol dm^{-3} [(*f*)]: $[Mn^{II}]$ = 0.05 [(*a*)–(*c*)], 0.025 mol dm^{-3} [(*d*)–(*h*)]; $[Mn^{III}]$ = 0.05 [(*a*)–(*e*), (*g*), (*h*)], $[^{-}ON(NO)SO_3^{-}]$ = 0.2 [(*a*)], 2 [(*b*)], 4 [(*g*)], 6 [(*c*), (*d*), (*f*), (*h*)], 8 mmol dm^{-3} [(*e*)]

the influence of pH, $[Mn^{II}]$ and $[Mn^{III}]$ was studied. In the absence of O_2 only the reduction of $Mn^{III}(N_3)^{2+}$ to Mn^{II} could be observed [Fig. 10(*a*) and 10(*b*)]. The fast and slow reactions in Fig. 10(*b*) are not so uncommon for the reduction of $Mn^{III}(N_3)^{2+}$ by nitrogen–sulfur oxides. We have reported in detail on the mechanism by which $Mn^{III}(N_3)^{2+}$ is reduced by different nitrogen–sulfur compounds[26] and found similar complications for S^{IV}, $HN(SO_3)_2^{2-}$ and $ON(SO_3)_3^{3-}$. The two steps observed were interpreted either in terms of a rate-determining substitution of a H_2O or N_3^{-} ligand on the manganese(III) species followed by a rapid electron-transfer reaction, or by a slow intramolecular electron-transfer reaction following the rapid formation of a manganese(III)–nitrogen–sulfur complex. In the presence of O_2 the absorbance traces look completely different (Fig. 11). An increase in $[Mn^{III}]$ as a function of time is observed. When the $[^{-}ON(NO)SO_3^{-}]$ is low only oxidation of Mn^{II} to Mn^{III} can be observed. Upon increasing the $[^{-}ON(NO)SO_3^{-}]$, Mn^{II} is first oxidized to Mn^{III} and then a further build-up of Mn^{III} is preceded by an induction period. Upon increasing the $[^{-}ON(NO)SO_3^{-}]$ further the induction period becomes a complete reaction step consisting of a decrease and increase in Mn^{III}. When $[Mn^{II}]$ is lowered the first reduction step can be observed at low dianion concentrations. This step probably consists of simultaneous oxidation and reduction of Mn^{II} and Mn^{III}, respectively. Upon increasing $[Mn^{III}]$ and pH, the complete redox cycle proceeds over a shorter reaction time.

Suggested Mechanism.—At high pH the formation of $HON(SO_3)_2^{2-}$, $^{-}ON(NO)SO_3^{-}$ and sulfite during the reaction of $HONH(SO_3)^{-}$ with Mn^{II} can be explained in terms of the spontaneous hydrolysis of $HONH(SO_3)^{-}$ [reaction (1)] and the Boedeker-type reaction outlined in Scheme 2.[28] The overall reaction results in the oxidation of Mn^{II} to Mn^{III} as in Fig. 2. A simulation of the observed kinetic traces is not possible due to a lack of information on the rate constants of the various reaction steps in Scheme 2 (see further Discussion). Evidence for the formation of $Mn^{II}(NO)^{2+}$ has been reported.[50]

$$^{-}ON(NO)SO_3^{-} \rightleftharpoons NOSO_3^{2-} + NO$$

$$^{-}ON(NO)SO_3^{-} \rightleftharpoons SO_3^{2-} + 2NO$$

$$Mn^{II} + NO \longrightarrow Mn^{II}(NO)^{2+}$$

$$Mn^{II}(NO)^{2+} + SO_3^{2-} \longrightarrow Mn(ONSO_3) \xrightarrow{SO_3^{2-}} HON(SO_3)_2^{2-}$$

$$\downarrow$$

$$Mn^{III} + NO^{-} + SO_3^{2-}$$
$$(N_2O)$$

Scheme 2

At low pH in azide media the results indicate that the oxidation of Mn^{II} to Mn^{III} is preceded by complex formation between Mn^{II} and $^{-}ON(NO)SO_3^{-}$. In agreement with our results on the sulfite-induced autoxidation of Mn^{II},[21] as well as those recently published elsewhere,[1] the $^{-}ON(NO)SO_3^{-}$-induced autoxidation of Mn^{II} is affected autocatalytically by Mn^{III}, and no significant oxidation is observed in the absence of initially added Mn^{III}. Based on this result the overall mechanism is suggested to follow the reactions outlined in Scheme 3. This reaction sequence involves very similar steps to those suggested

Table 1 Suggested mechanism and selected stability and rate constants used for the simulations in Fig. 12

Reaction	Stability or rate constant[a]	
	Lit. value	Value used in simulation
$Mn^{II} + {}^{-}ON(NO)SO_3^{-} \rightleftharpoons Mn^{II}\{ON(NO)SO_3\}$	2.7 ± 1.1[b,c]	2.4[c]
$Mn^{II}\{ON(NO)SO_3\} + Mn^{III} \longrightarrow 2Mn^{II} + 2NO + SO_3^{-}$	8×10^{2}[d]	5×10^{2}
$Mn^{III} + SO_3^{-} + H_2O \longrightarrow Mn^{II} + SO_4^{2-} + 2H^{+}$	1.5×10^{7}[e]	3.8×10^{8}
$SO_3^{-} + O_2 \longrightarrow SO_5^{-}$	$(1.1–2.5) \times 10^{9}$[e,f]	2.5×10^{9}
$Mn^{II} + SO_5^{-} + H^{+} \longrightarrow Mn^{III} + HSO_5^{-}$	*ca.* 10^{8}[f]	5×10^{8}
$Mn^{II} + HSO_5^{-} \longrightarrow Mn^{III} + SO_4^{2-} + OH$	Slow[f]	$< 1 \times 10^{4}$
$\longrightarrow Mn^{III} + SO_4^{-} + OH^{-}$	Slow[f]	$< 1 \times 10^{4}$
$Mn^{II} + SO_4^{-} \longrightarrow Mn^{III} + SO_4^{2-}$	3×10^{7}[f]	3×10^{7}
$Mn^{II} + OH + H^{+} \longrightarrow Mn^{III} + H_2O$	2.6×10^{7}[f]	2.6×10^{7}
${}^{-}ON(NO)SO_3^{-} + H^{+} \longrightarrow HSO_4^{-} + N_2O$	2×10^{4}[g]	4×10^{4}
$SO_5^{-} + SO_5^{-} \longrightarrow 2SO_4^{-} + O_2$	1×10^{7}–1×10^{9}[e,f]	1.1×10^{7}
$SO_5^{-} + SO_5^{-} \longrightarrow S_2O_8^{2-} + O_2$	1.4×10^{8}[f]	5×10^{7}
$SO_3^{-} + SO_3^{-} \longrightarrow S_2O_6^{2-}$	1.8×10^{8}–2.3×10^{9}[e,f]	2.5×10^{8}

[a] In units of $dm^3\ mol^{-1}\ s^{-1}$ unless otherwise stated. [b] Mean value of various complex-formation constants of Mn^{II} reported in ref. 40. [c] In units of $dm^3\ mol^{-1}$. [d] Experimental value measured at pH 6, 25 °C, I = 1.0 mol dm^{-3}, $[Mn^{III}] = 5 \times 10^{-5}$ mol dm^{-3} and $[N_3^{-}]_T$ = 0.5 mol dm^{-3}. [e] Data quoted in ref. 51. [f] Data quoted in ref. 1. [g] Data taken from refs. 35–37 and converted into a second-order rate constant for the acid-catalysed reaction.

$$Mn^{II} + {}^{-}ON(NO)SO_3^{-} \rightleftharpoons Mn^{II}\{ON(NO)SO_3\}$$

$$Mn^{II}\{ON(NO)SO_3\} + Mn^{III} \longrightarrow 2Mn^{II} + ON(NO)SO_3^{-}$$

$$ON(NO)SO_3^{-} + Mn^{III} + H_2O \longrightarrow 2NO + SO_4^{2-} + 2H^{+} + Mn^{II}$$

$$ON(NO)SO_3^{-} + O_2 \longrightarrow ON(NO)SO_5^{-}$$

$$Mn^{II} + ON(NO)SO_5^{-} \xrightarrow{H^{+}} Mn^{III} + ON(NO)HSO_5^{-}$$

$$Mn^{II} + ON(NO)HSO_5^{-} \longrightarrow Mn^{III} + N_2O + OH^{-} + SO_5^{-}$$

$$Mn^{II} + SO_5^{-} \xrightarrow{H^{+}} Mn^{III} + HSO_5^{-}$$

$$Mn^{II} + HSO_5^{-} \longrightarrow Mn^{III} + OH^{-} + SO_4^{-}$$

$$Mn^{II} + SO_4^{-} \longrightarrow Mn^{III} + SO_4^{2-}$$

Scheme 3

before to account for the redox cycling of $Mn^{II/III}$ under such conditions in the presence of sulfite and oxygen.[1,21] The difference in the present system is that ${}^{-}ON(NO)SO_3^{-}$ is the species responsible for the redox cycling, and we therefore include the formation of an oxidized $ON(NO)SO_3^{-}$ species which can react rapidly with molecular oxygen to produce a peroxomonosulfate analogue. This species is presumably a strong oxidant (similar to SO_5^{-}) and can induce the oxidation of Mn^{II} as shown in the subsequent reactions. It also involves the formation of SO_5^{-} radicals which follows the reaction sequence suggested before.[20,22,51] Scheme 3 can in principle account for a single redox cycle of $Mn^{II/III}$, in which the initial presence of some Mn^{III} leads to the production of $ON(NO)SO_3^{-}$ which induces the autoxidation of Mn^{II} in the subsequent reaction steps. The ${}^{-}ON(NO)SO_3^{-}$:O_2 ratio determines whether oxidation of Mn^{II} or reduction of Mn^{III} will occur, as reported in the case of sulfite.[21] At higher concentrations of ${}^{-}ON(NO)SO_3^{-}$ the reduction to Mn^{II} will be favoured, whereas at lower concentrations an overall oxidation of Mn^{II} will be observed.

The results in Fig. 11 clearly demonstrate that under certain experimental conditions up to two redox cycles are observed. A similar result was observed in the corresponding sulfite system.[21] This is in the present case probably due to two possible redox steps, one between Mn^{III} and ${}^{-}ON(NO)SO_3^{-}$ co-ordinated to Mn^{II} at low $[Mn^{III}]$, and another directly

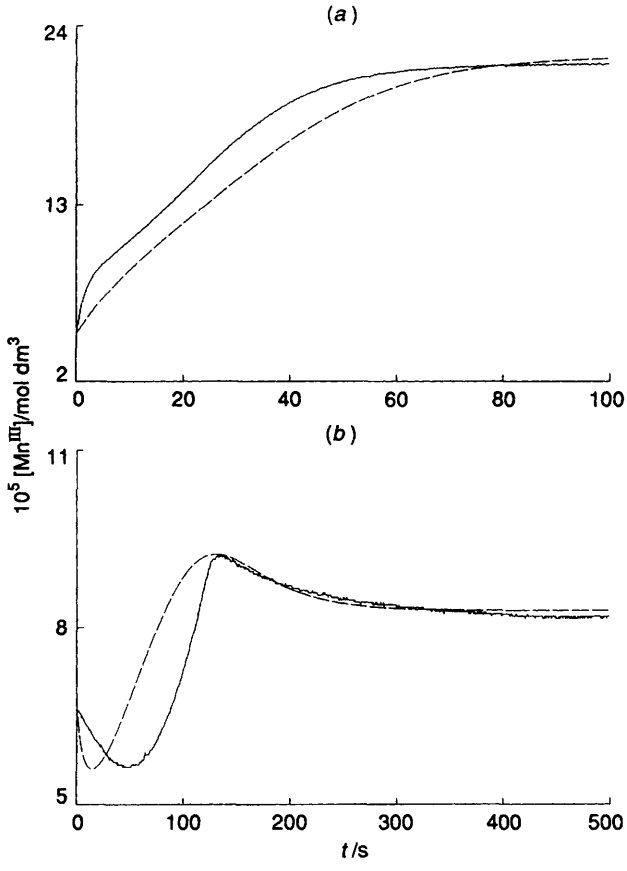

Fig. 12 Simulated (– – –) kinetic traces based on the mechanism and constants given in Table 1 for the experimental conditions in (*a*) Fig. 11(*b*) and (*b*) Fig. 11(*c*)

between Mn^{III} and the dianions at higher $[Mn^{III}]$. Thus, as Mn^{III} is formed during the ${}^{-}ON(NO)SO_3^{-}$-induced autoxidation of Mn^{II}, the latter reaction can account for the second redox cycle. Alternatively, the reactions in Scheme 3 contain two species which can induce the autoxidation process, *viz.* $ON(NO)SO_5^{-}$ and SO_5^{-}. It follows that, under particular conditions, the formation of SO_5^{-} (and subsequently HSO_5^{-} and SO_4^{-}) could account for the second redox cycle of $Mn^{II/III}$.

We conclude that the general mechanism outlined in Scheme

3 can in principle account qualitatively for the observed kinetic traces. At present not enough information on the various reaction steps is available to allow a more quantitative treatment. If we assume that the intermediate $ON(NO)SO_3^-$ species decomposes spontaneously to NO and SO_3^-, a modified reaction scheme with more known constants can be derived (see Table 1). Simulations on the basis of this scheme using the ZITA program[52] for some of the experimental conditions of Fig. 11 are reported in Fig. 12. The simulated kinetic traces are in close agreement with those found experimentally, from which it follows that the suggested scheme in Table 1 can in principle account for the type of kinetic traces in Fig. 11. Efforts to simulate the redox cycling of $Mn^{II/III}$ in the presence of $^-ON(NO)SO_3^-$ and oxygen under other experimental conditions will be continued and more details on these types of reaction mechanisms should be forthcoming.

Acknowledgements

We gratefully acknowledge financial support from the Bundesministerium für Forschung und Technologie, VEBA Kraftwerke Ruhr and a stipend from Deutscher Akademischer Austauschdienst (to F. F. P.).

References

1 J. Berglund, S. Franaeus and L. I. Elding, *Inorg. Chem.*, 1993, **32**, 4527.
2 A. Huss, P. K. Lim and C. A. Eckert, *J. Phys. Chem.*, 1982, **86**, 4229.
3 T. Ibusuki and H. M. Barnes, *Atmos. Environ.*, 1984, **18**, 145.
4 L. A. Barrie and H. W. Georgi, *Atmos. Environ.*, 1976, **10**, 743.
5 P. W. Cains and M. D. Carabine, *J. Chem. Soc., Faraday Trans. 1*, 1978, 2689.
6 H. Bassett and W. G. Parker, *J. Chem. Soc.*, 1951, 1540.
7 D. Littlejohn and Y. Z. Wang, *Ind. Eng. Chem. Res.*, 1990, **29**, 10.
8 S. Mukhopadhyay and R. Banerjee, *J. Chem. Soc., Dalton Trans.*, 1993, 933.
9 P. A. Siskos, V. C. Peterson and R. E. Huie, *Inorg. Chem.*, 1984, **23**, 1134.
10 G. Davies, L. J. Kirschenbaum and K. Kustin, *Inorg. Chem.*, 1969, **8**, 663.
11 D. Littlejohn and S.-G. Chang, *Energy Fuels*, 1991, **5**, 249.
12 T. K. Ellison and C. A. Eckert, *J. Phys. Chem.*, 1984, **88**, 2335.
13 W. Weisweiller, R. Blumehofer, B. N. Avasthi and S. K. Srivastava, *Proceedings of National Seminar on Environmental Pollution and Control in Mining, Coal and Mineral Based Industries*, Indian Institute of Technology, Madras, 1987, p. 251.
14 S.-G. Chang, R. Toossi and T. Novakov, *Atmos. Environ.*, 1981, **15**, 1287.
15 K. Bal Reddy and R. van Eldik, *Atmos. Environ.*, 1992, **26**, 661.
16 J. Kraft and R. van Eldik, *Inorg. Chem.*, 1989, **28**, 2297.
17 J. Kraft and R. van Eldik, *Inorg. Chem.*, 1989, **28**, 2306.
18 J. Kraft and R. van Eldik, *Atmos. Environ.*, 1989, **23**, 2709.
19 K. Bal Reddy, N. Coichev and R. van Eldik, *J. Chem. Soc., Chem. Commun.*, 1991, 481.
20 N. Coichev and R. van Eldik, *Inorg. Chem.*, 1991, **30**, 2375.
21 N. Coichev and R. van Eldik, *Inorg. Chim. Acta*, 1991, **185**, 69.
22 R. van Eldik, N. Coichev, K. Bal Reddy and A. Gerhard, *Ber. Bunsenges. Phys. Chem.*, 1992, **96**, 478.
23 S. Yamamoto and T. Kaneda, *J. Chem. Soc. Jpn.*, 1959, **80**, 1098.
24 S. B. Oblath, S. S. Markowitz, T. Novakov and S.-G. Chang, *J. Phys. Chem.*, 1981, **85**, 1017.
25 S. B. Oblath, S. S. Markowitz, T. Novakov and S.-G. Chang, *J. Phys. Chem.*, 1982, **86**, 4853.
26 F. F. Prinsloo, J. J. Pienaar, R. van Eldik and H. Gutberlet, *J. Chem. Soc., Dalton Trans.*, 1994, 2373.
27 J. H. Swinehart, *Coord. Chem. Rev.*, 1967, **2**, 385.
28 V. Zang and R. van Eldik, *J. Chem. Soc., Dalton Trans.*, 1993, 111.
29 J. P. Candlin and R. G. Wilkins, *J. Am. Chem. Soc.*, 1965, **87**, 1490.
30 S. B. Oblath, S. S. Markowitz, T. Novakov and S.-G. Chang, *Inorg. Chem.*, 1983, **22**, 579.
31 D. Littlejohn, K. Y. Hu and S.-G. Chang, *Inorg. Chem.*, 1985, **25**, 3131.
32 D. Littlejohn and S.-G. Chang, *Ind. Eng. Chem. Res.*, 1990, **29**, 10.
33 S. Nyholm and L. Rannitt, *Inorg. Synth.*, 1967, 1718.
34 M. Geissler and R. van Eldik, *Anal. Chem.*, 1992, **64**, 3004.
35 F. Seel and R. Winkler, *Z. Naturforsch., Teil A*, 1963, **18**, 155.
36 M. N. Ackermann and R. E. Powell, *Inorg. Chem.*, 1967, **6**, 1718.
37 D. Littlejohn, K. Y. Hu and S.-G. Chang, *Inorg. Chem.*, 1986, **25**, 3131.
38 J. J. Morgan, in *Principles and Applications of Water Chemistry*, eds. S. D. Faust and J. V. Hunter, Wiley, New York, 1967, p. 561; F. F. Prinsloo, J. J. Pienaar and R. van Eldik, unpublished work.
39 M. Monfort, J. Ribas and X. Solans, *J. Chem. Soc., Chem. Commun.*, 1993, 350.
40 L. G. Sillen and A. E. Martell (Editors), *Stability Constants of Metal–Ion Complexes*, Special Publ., No. 17, The Chemical Society, London, 1989.
41 C. Brandt, N. Coichev, E. Hostert and R. van Eldik, *GIT Fachz. Lab.*, 1993, **4**, 277.
42 E. Sada and H. Kumazawa, *Ind. Eng. Chem., Process Des. Dev.*, 1980, **19**, 377.
43 E. Sada and H. Kumazawa, *Ind. Eng. Chem., Process Des. Dev.*, 1981, **20**, 46.
44 G. F. Wells and G. Davies, *J. Chem. Soc. A*, 1967, 1858.
45 *Gmelins Handbuch der anorganischen Chemie*, Verlag Chemie, Weinheim, 1973, vol. 56, Part C1, p. 366.
46 T. E. Jones and R. E. Hamm, *Inorg. Chem.*, 1975, **14**, 1027.
47 Y. N. Lee and S. E. Schwartz, *J. Geophys. Res.*, 1981, **86**, 971.
48 M. N. Ackermann and R. E. Powell, *Inorg. Chem.*, 1966, **25**, 3131.
49 J. P. Candlin and R. G. Wilkins, *J. Am. Chem. Soc.*, 1965, **87**, 1490.
50 G. Hüfner, *Z. Phys. Chem.*, 1907, **59**, 416.
51 C. Brandt, I. Fabian and R. van Eldik, *Inorg. Chem.*, 1994, **33**, 687.
52 G. Peintler, ZITA 3.0, A comprehensive program package for fitting parameters of chemical reaction mechanisms, Szeged, 1992.

Received 11*th May* 1994; *Paper* 4/02797C